

## TRANSVERSE FATIGUE CHARACTERISTICS OF BOLTED JOINTS TIGHTENED THIN PLATES

Shinji Hashimura<sup>(\*)</sup>, Jyunpei Maekawa, Takuya Niiyama

Department of Engineering Science and Mechanics, Shibaura Institute of Technology, Tokyo, Japan

<sup>(\*)</sup>*Email:* hasimura@shibaura-it.ac.jp

### ABSTRACT

Bolted joints subjected to vibrations in service have been always exposed risks of self-loosening and fatigue failure. However the occurrence conditions of transverse bolt fatigue have not been sufficiently revealed although many researches with regard to axial bolt fatigue were performed. We had investigated the self-loosening and fatigue characteristics of bolted joints subjected to transverse vibration in our previous study. At this time, grip length, that is a clamping length due to the bolt, was comparatively long. In this study, transverse fatigue tests of the bolted joints with short grip length to simulate a thin plate tightening structure. Influences of the grip length and the engaging thread length on apparent transverse fatigue limits that is the highest amplitude of transverse vibration in which the bolt does not break due to fatigue, have been investigated. The results showed that the apparent transverse fatigue limits decreased with an increase in the grip length and the engaging thread length.

**Keywords:** bolted joint, fatigue, transverse vibration, grip length, engaging thread length.

### INTRODUCTION

Bolted joint corruptions often cause serious accidents in vehicles and structures (Ministry of Land, Infrastructure and Transport, 2013) (Asahi Shinbun, 2002). It is generally considered that the causes of the corruptions are self-loosening and fatigue failures of the bolts (Kasei, 1989) (Hess, 1996) (Hess, 1997) (Pai, 2002) (Jiang, 2003) (Zhang, 2006). Hence we have to avoid the self-loosening and the fatigue failures when we use the bolted joints. The bolted joints used in the machines and structures subjected to transverse vibrations in service have been always exposed higher risks of self-loosening and fatigue failure in particularly. However the occurrence conditions of fatigue failure of bolted joint subjected to transverse vibration have not been sufficiently revealed although many researches with regard to fatigue failure of bolted joint subjected to axial vibration were performed (Stephens, 2007) (Alexander, 2000) (Yoshimoto, 1984) (Ohashi, 1985) (Ohashi, 1994). In our previous researches so far, we have mainly investigated the fatigue characteristics of bolted joints under transverse vibration (Hashimura, 2006) (Hashimura, 2007) (Hashimura, 2010). The grip length, that is a clamping length due to the bolt, was from four times to five times of the bolt size approximately, that was comparatively long. If the bolted joints have a comparative long such as the previous experiments, the bolt broke due to bending moment by means of transverse vibration force. Since the bending moment was a multiplication of the grip length and transverse vibration force, it had been seen that the apparent transverse fatigue limits, that is the highest amplitude of transverse vibration in which the bolt does not break due to fatigue, depended on the grip length. However the bolts might break due to shear force if grip length was short.

In this study, transverse fatigue tests of the bolted joints with comparatively short grip length to simulate a thin plate structure have been conducted. The grip lengths were from the almost same length as the bolt size to about twice of the bolt size. Influences of the grip length and the engaging thread length on apparent transverse fatigue limits have been investigated in the fatigue tests. The bolts used in the tests were commercial hexagon head bolt.

**TEST BOLTS AND TIGHTENING SITUATIONS**

Figure 1 shows the schematic illustrations of test bolts and the tightening situations. In the experiments, six types of bolts with different nominal lengths were used. Each test bolt was a commercial hexagon head bolt M10 with thread pitch 1.5 mm and with fully threaded, and the bolt property class was 8.8. Table 1 shows the mechanical properties of the test bolts (Yamamoto, 1996). The test bolt was tightened into an internal thread adaptor in the experimental apparatus before the transverse fatigue test. The tightening situations shown in Fig. 1(a) were for investigation of an influence of the grip length  $l_g$  on the apparent fatigue limits. Fig. 1(b) shows the tightening situations to investigate influences of two engaging thread length  $l_e$  on the apparent fatigue limits.

Table 1 - Mechanical properties of test bolt (property class: 8.8)

Young's modulus $E$	Ultimate Strength $\sigma_u$	Proof Stress $\sigma_{0.2}$	True Ultimate Strength of Bolt Material $\sigma_T$	Fatigue Strength of Bolt Material $\sigma_{w0}$	Notch factor at the root of the first thread $K_\phi$
206 GPa	800 MPa	640 MPa	1370 MPa	290 MPa	3.56

In Fig. 1(a), the engaging thread length was  $l_e = 15$  mm constant. The grip lengths were  $l_g = 9$  mm, 12 mm, 17 mm and 22 mm respectively. In Fig. 1(b), the grip lengths were  $l_g = 9$  mm and 17 mm. The engaging thread lengths were  $l_e = 10$  mm, 15 mm and 20 mm respectively. As can be seen that the nominal lengths  $l$  of the bolts were different for each tightening situation. Hence the bolts were manufactured cutting the bolts with  $l = 40$  mm in order to prepare the test bolts from the same lot. The corners of the bearing surface of all the bolts were machined with a lathe to create a flat contact surface as shown in Fig.1.

$l$ : Nominal length,  $l_g$ : Grip length,  $l_e$ : Engaging thread length

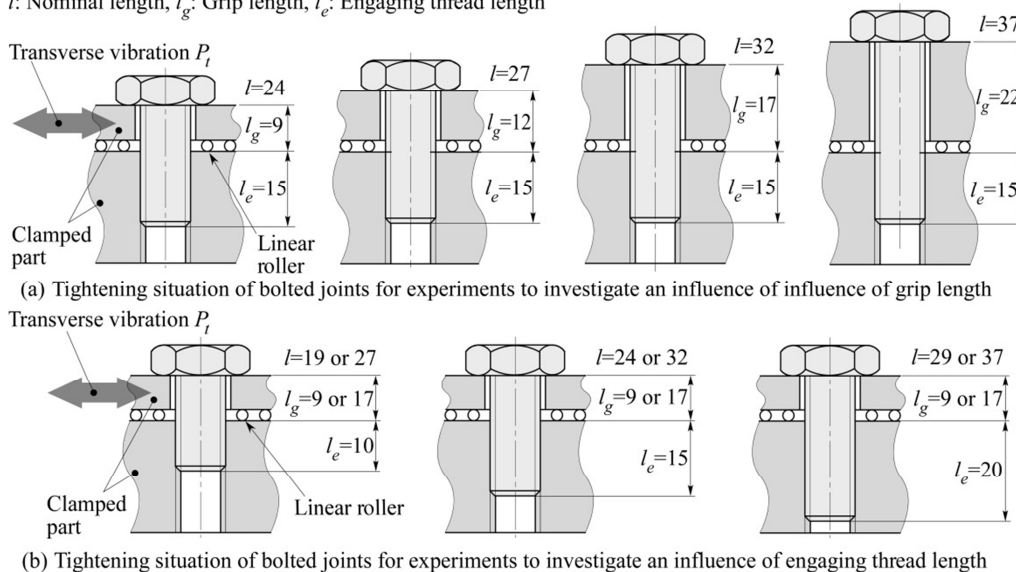


Fig. 1 - Test bolts and tightening situations for the transverse fatigue test of bolted joints

Incidentally, there are linear rollers between two clamped parts in Fig. 1(a) and Fig. 1(b) although actual bolted joints do not have the linear rollers. In the experiments, the linear rollers were placed in order to ignore friction losses between the clamped parts. Consequently the bolt had directly received the transverse force through the bearing surface of the bolt.

## EXPERIMENTAL APPARATUS

Figure 2 shows a schematic illustration of an apparatus for the transverse fatigue tests. The apparatus was designed to simulate a two-plate structure without a nut. In Fig.2, the test bolt was tightened into the internal thread adaptor, with its rotation fixed on a fixed clamped part, through a bearing surface part and a load cell for measuring the clamping force  $F$  located in the center of the apparatus. The lower clamped part including the load cell was fixed on the base plate and the upper clamped part was vibrated with an air vibrator. The transverse vibration force  $\Delta P_t/2$  was controlled by air pressure applied to the air vibrator, with a constant amplitude load. The frequency of the vibration depended on the air pressure, and varied from 35 Hz to 50 Hz.

The contact surfaces between the two clamped parts were hardened and two lubricated linear rollers were placed between the clamped parts in order to ignore the friction. Frictional losses were measured to be less than 1% of the transverse vibration force  $\Delta P_t/2$  and were ignored in this study. The displacement  $\delta$  of the vibrated clamped part was measured by a laser displacement transducer during the transverse fatigue test.

An internal thread adaptor was made of a medium carbon steel JIS S55C and the internal thread was manufactured by tapping. A tap was inserted into the thread before each experiment. If an abnormality of the internal thread was detected, the adaptor was replaced with a new one. Otherwise, the adaptor was repeatedly used in the experiments. The bearing surface part was also made of a medium carbon steel JIS S55C. The bearing surface contacting the bolt head was polished with #600 sand paper before each experiment. A washer was not used in the experiments.

## EXPERIMENTAL PROCEDURE

In the transverse fatigue tests, the test was started after the test bolt was tightened using a wrench at  $F_t=15\text{kN}$ . It was stopped when the clamping force  $F$  reached zero or the loading

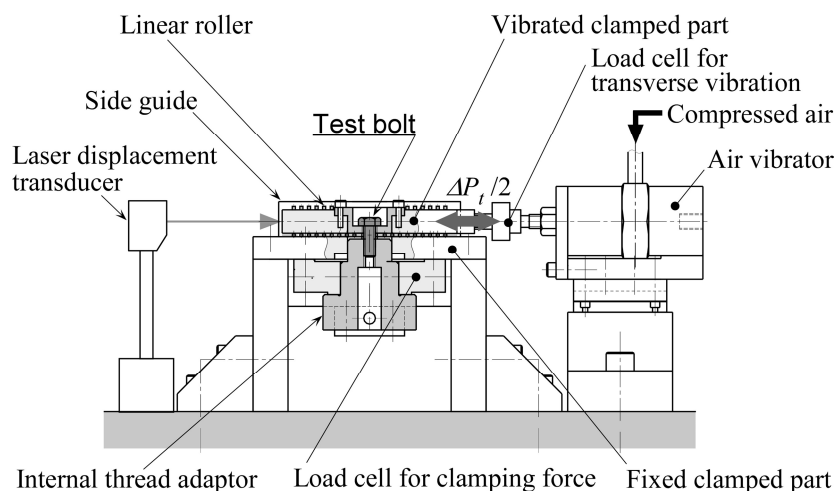


Fig. 2 - An experimental apparatus for the transverse fatigue test of bolted joints

cycles exceeded ten million cycles. The initial clamping force  $F_i=15\text{kN}$  corresponds to the elastic region of the test bolts. In all experiments, the thread surface and bearing surface were lubricated by Molybdenum disulfide grease. In the transverse fatigue test, we could find a higher threshold of the amplitude  $\Delta P_t/2$  of transverse vibration force at which the bolt does not break due to fatigue. In this study, we defined the thresholds as the apparent transverse fatigue limit  $(\Delta P_t/2)_w$ .

### INFLUENCE OF GRIP LENGTH ON APPARENT FATIGUE LIMIT

Figure 3 shows behaviours of clamping forces  $F$  for each amplitude  $\Delta P_t/2$  of transverse vibration force. In these experiments, the grip length was  $l_g=17\text{ mm}$  and the engaging thread length was  $l_e=15\text{ mm}$ . In Fig. 3, the ordinate is the clamping force  $F$  and the abscissa is the number of cycle  $N$  of the transverse vibration force.

It can be seen in Fig.3  $\Delta P_t/2=0.55\text{ kN}$  that the clamping forces  $F$  rapidly decreased after the clamping force  $F$  had kept a constant value for a while. When the amplitude of transverse vibration force was  $\Delta P_t/2=0.55\text{ kN}$  in Fig. 3, the clamping force  $F$  did not almost decrease. The bolt which the clamping force  $F$  was completely lost in this study had fatigue cracks at the neck portion under the bolt head, the root of the incomplete thread or the root of the first thread. For these bolt which the clamping force  $F$  was completely lost, the number of cycle  $N_f$  to failure significantly depended on the amplitude  $\Delta P_t/2$  of transverse vibration force.

Figure 4 shows relationships between the amplitude of transverse vibration force  $\Delta P_t/2$  and the number of cycle  $N_f$  to failure in the experiments to investigate an influence of the grip length. In Fig. 4, the ordinate is  $\Delta P_t/2$  and the abscissa is  $N_f$ . Symbols  $\blacklozenge, \blacktriangle, \blacksquare, \bullet$  indicate the result for  $l_g=22\text{ mm}, 17\text{ mm}, 12\text{ mm}$  and  $9\text{ mm}$  respectively. The white color symbols show indicate the results which the bolts did not break without clamping force reduction.

It can be seen in Fig. 4 that the fatigue lives  $N_f$  depends the amplitude of transverse vibration force  $\Delta P_t/2$ . And the apparent transverse fatigue limits  $(\Delta P_t/2)_w$  decreased with an increase in

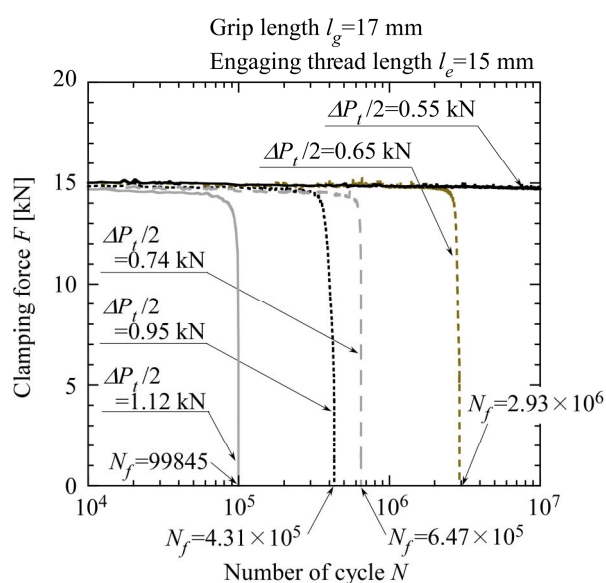


Fig. 3 - Variations of clamping force of the bolted joints during the transverse fatigue tests

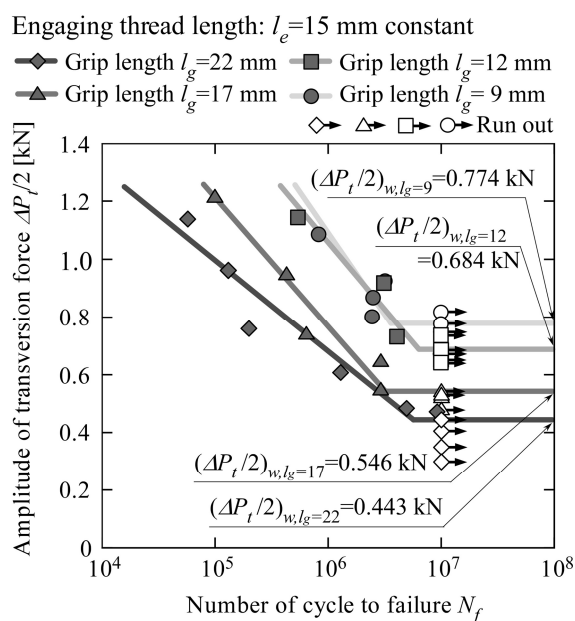


Fig. 4 - Relationships between amplitudes of transverse force  $\Delta P_t/2$  and number of cycles to failure  $N_f$ .

the grip length  $l_g$ . In the experiments, main fatigue cracks of the broken bolt had been generated at the root of the incomplete thread or the neck under the bolt head. However the all main fatigue cracks of the broken bolt due to  $\Delta P_t/2$  just above  $(\Delta P_t/2)_w$  were generated at the root of the incomplete thread of bolt.

Figure 5 shows a relationship between the apparent transverse fatigue limits  $(\Delta P_t/2)_w$  and the the grip length  $l_g$ . Fig. 5(a) shows the relationship between  $(\Delta P_t/2)_w$  and  $l_g$ . Fig. 5(b) shows fracture surfaces and fatigue cracks of the broken bolt at the root of the incomplete thread. In the experiments, since positions at which main fatigue cracks of the broken bolt due to  $\Delta P_t/2$  just above  $(\Delta P_t/2)_w$  occurred were different in accordance with the tightening conditions such as the grip length and the engaging thread length, the positions was wrote in the side of the experimental points in Fig. 5(a). It can be seen in Fig. 5 that the apparent transverse fatigue limits  $(\Delta P_t/2)_w$  were in completely proportion to the grip length  $l_g$ .

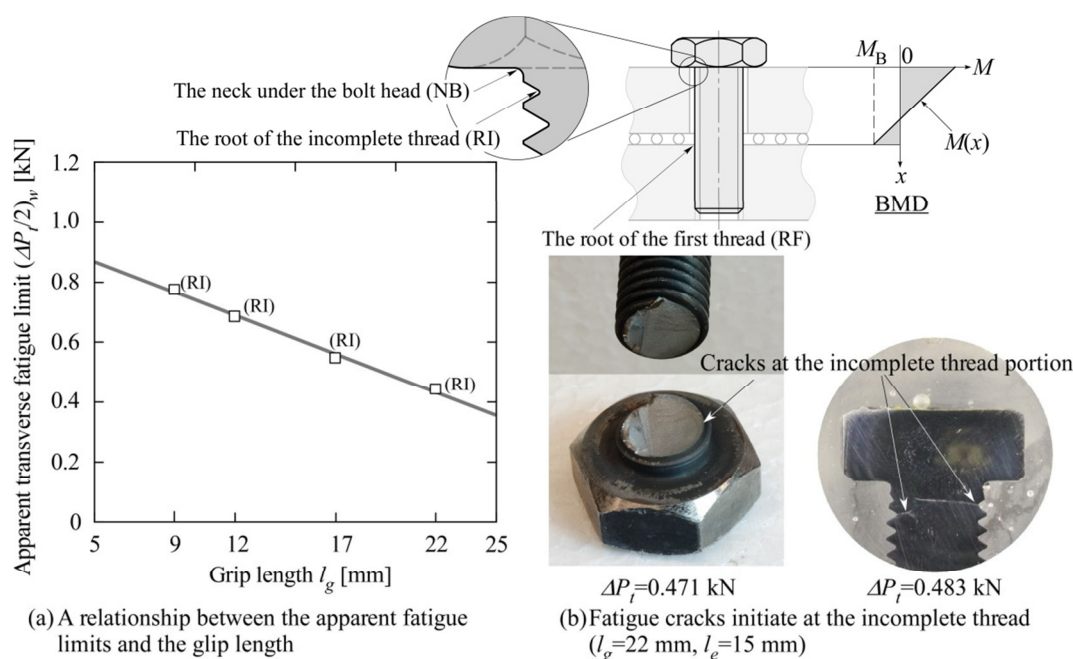


Fig. 5 - Graph of relationships between apparent fatigue limits  $(\Delta P_t/2)_w$  and grip length  $l_g$  and fracture surfaces and typical fatigue cracks nucleated at the incomplete thread of the bolt.

In our previous study, if the grip length of the bolted joint was comparatively long, it was revealed that the bolt broke due to the bending moment which the bolt was loaded. Fig.6 shows a schematic illustration of a deformed bolt due to the transverse vibration force  $\Delta P_t/2$  and a bending moment diagram of the bolt. As can be seen in Fig. 6, the bolt deforms S-shape if the bolt was loaded transverse force  $P_t$ . The bending moment diagram at this case can be drawn such as the right diagram of Fig. 6.

Let  $x$  be the bolt axial position in Fig. 6, the bending moment  $M(x)$  is expressed the following equation.

$$M(x) = (\Delta P_t/2) \cdot x - M_B \quad (1)$$

where  $M_B$  is the bending moment generated due to constraint in transverse direction by the engaging threads and is expressed as a follows:

$$M_B = C \cdot (\Delta P_t/2) \cdot l_g \quad (2)$$

where  $C$  is a coefficient which is determined by constraint due to the engaging threads and by a slippage between thread surfaces.

As can be seen in Eq.(1) and (2), the bending moment  $M$  is in proportion to the grip length  $l_g$  regardless of fracture position. Therefore even if the bolted joints receive the same amplitude of transverse vibration, it is indicated that the bending moment  $M$  which the bolt is loaded changed if the grip lengths  $l_g$  are different. The results shown in Fig. 5(a) indicate that the test bolts in each grip length  $l_g$  broke due to not shearing force but the bending stress.

### INFLUENCE OF ENGAGING THREAD LENGTH ON APPARENT FATIGUE LIMIT

Figure 7 and 8 show relationships between the amplitude of transverse vibration force  $\Delta P_t/2$  and the number of cycle  $N_f$  to failure in the experiments to investigate influences of the

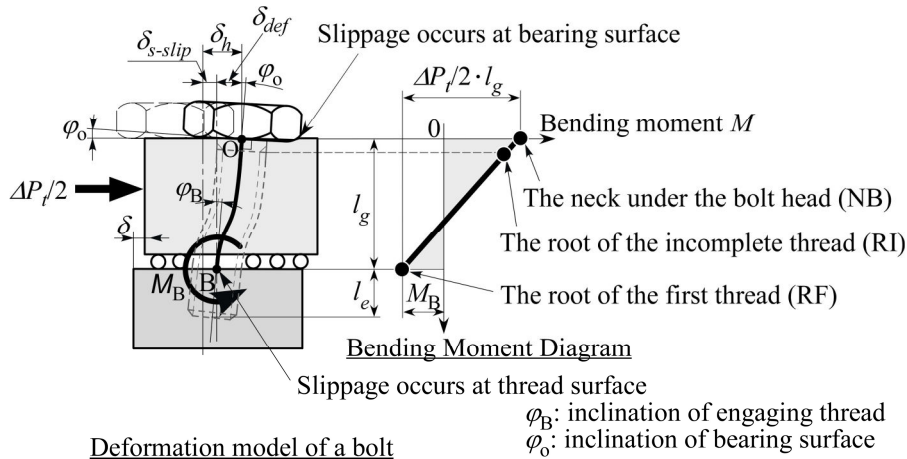


Fig. 6 - An illustration of the deformed bolt by transverse force and a bending moment diagrams of the bolt.

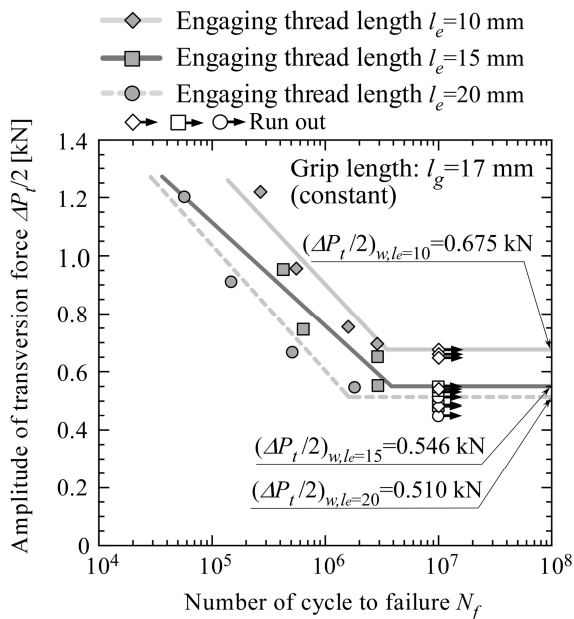


Fig. 7 - Relationships between amplitudes of transverse force  $\Delta P_t/2$  and number of cycles to failure  $N_f$ . (Investigation for an influence of  $l_e$ )

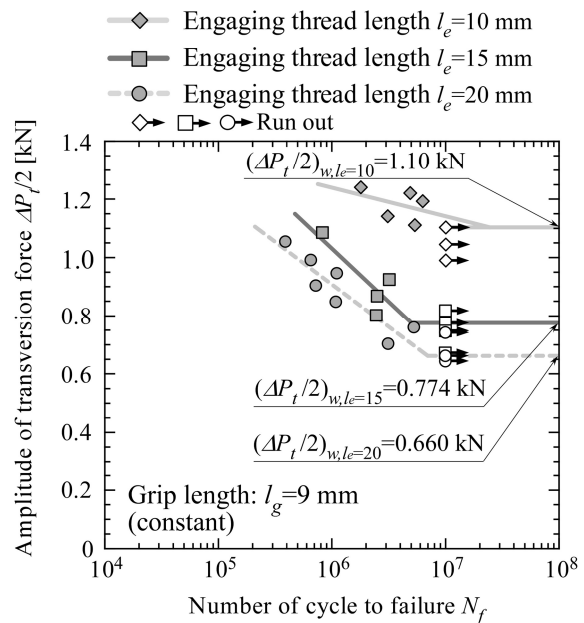


Fig. 8 - between amplitudes of transverse force  $\Delta P_t/2$  and number of cycles to failure  $N_f$ . (Investigation for an influence of  $l_e$ )

engaging thread length with the two grip length  $l_g$ . Fig. 7 was the results for  $l_g=17$  mm and Fig. 8 was the results for  $l_g=9$  mm. In Fig. 7 and 8, the ordinate is  $\Delta P_t/2$  and the abscissa is  $N_f$ . Symbols  $\blacklozenge$ ,  $\blacksquare$ ,  $\bullet$  indicate the result for  $l_e=10$  mm, 15 mm and 20 mm respectively. The white color symbols show of them are the results which the bolts did not break without clamping force reduction.

It can be seen in Fig. 7 that a difference between the apparent transverse fatigue limits  $(\Delta P_t/2)_w$  for  $l_e=15$  mm and  $(\Delta P_t/2)_w$  for  $l_e=20$  mm was small although a difference between  $(\Delta P_t/2)_w$  for  $l_e=10$  mm and  $(\Delta P_t/2)_w$  for  $l_e=15$  mm was large. In any case, if the engaging thread length  $l_e$  was long, the apparent transverse fatigue limit  $(\Delta P_t/2)_w$  decreased. In Fig. 8, a difference between  $(\Delta P_t/2)_w$  for  $l_e=15$  mm and  $(\Delta P_t/2)_w$  for  $l_e=20$  mm was not small. Meanwhile a difference between  $(\Delta P_t/2)_w$  for  $l_e=10$  mm and  $(\Delta P_t/2)_w$  for  $l_e=15$  mm was further large. In any case, if the engaging thread length  $l_e$  was long, the apparent transverse fatigue limit  $(\Delta P_t/2)_w$  decreased. Hence it is considered that the influence of the engaging thread lengths are magnified if the grip length was short.

Figure 9(a) shows relationships between the apparent transverse fatigue limits  $(\Delta P_t/2)_w$  and the engaging thread lengths  $l_e$ . Fig. 9(b) shows fracture surfaces and fatigue cracks of the broken bolt at the neck under the bolt head as a typical case although Fig. 9(b) is not the results shown in Fig. 7 and 8. Positions at which main fatigue crack of the broken bolt due to  $\Delta P_t/2$  just above  $(\Delta P_t/2)_w$  occurred was wrote in the side of the experimental points in Fig. 9(a). It can be seen in Fig. 9(a) that the apparent transverse fatigue limits  $(\Delta P_t/2)_w$  decreases with an increase in the engaging thread lengths  $l_e$ . But their relationships were not linear. The main fatigue cracks of the broken bolt due to  $\Delta P_t/2$  just above  $(\Delta P_t/2)_w$  of the case for  $l_e=10$  mm were different from other cases of  $l_e$ . A main fatigue crack generated at the neck under the bolt head in the case for  $l_g=9$  mm and  $l_e=10$  mm. In particularly in the case for  $l_g=17$  mm and  $l_e=10$  mm, two main fatigue cracks nucleated at the root of the incomplete thread and at the root of the first thread. It is considered from Fig. 9 that the bending moment diagrams of the bolts are changing according to each condition. To confirm the causes that the apparent

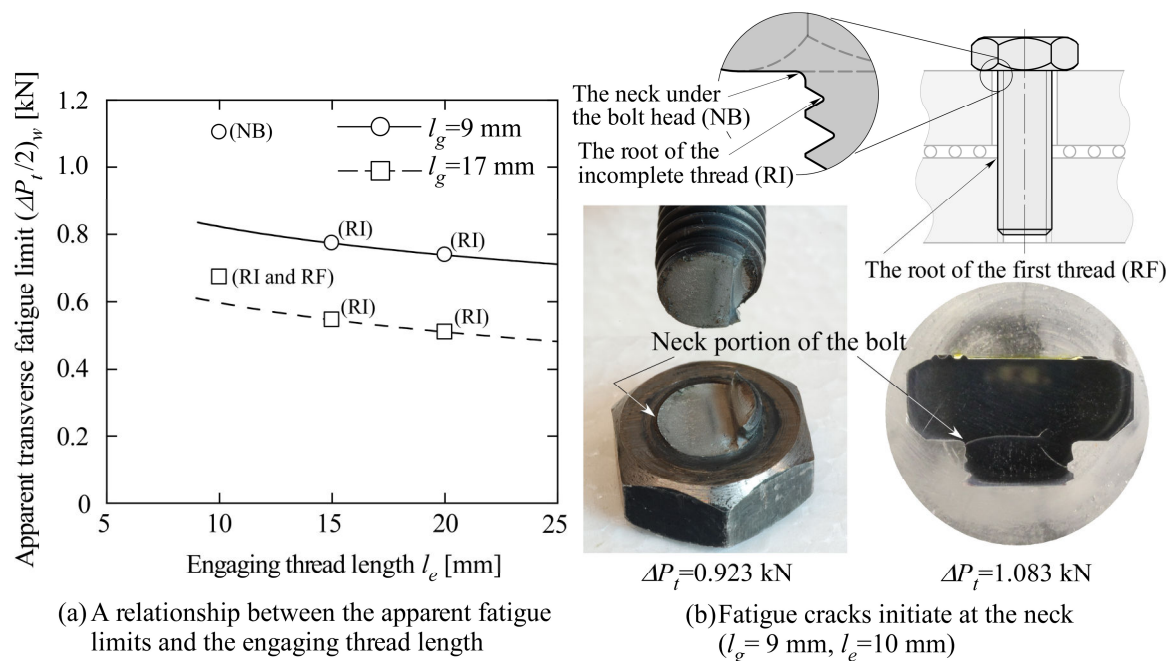
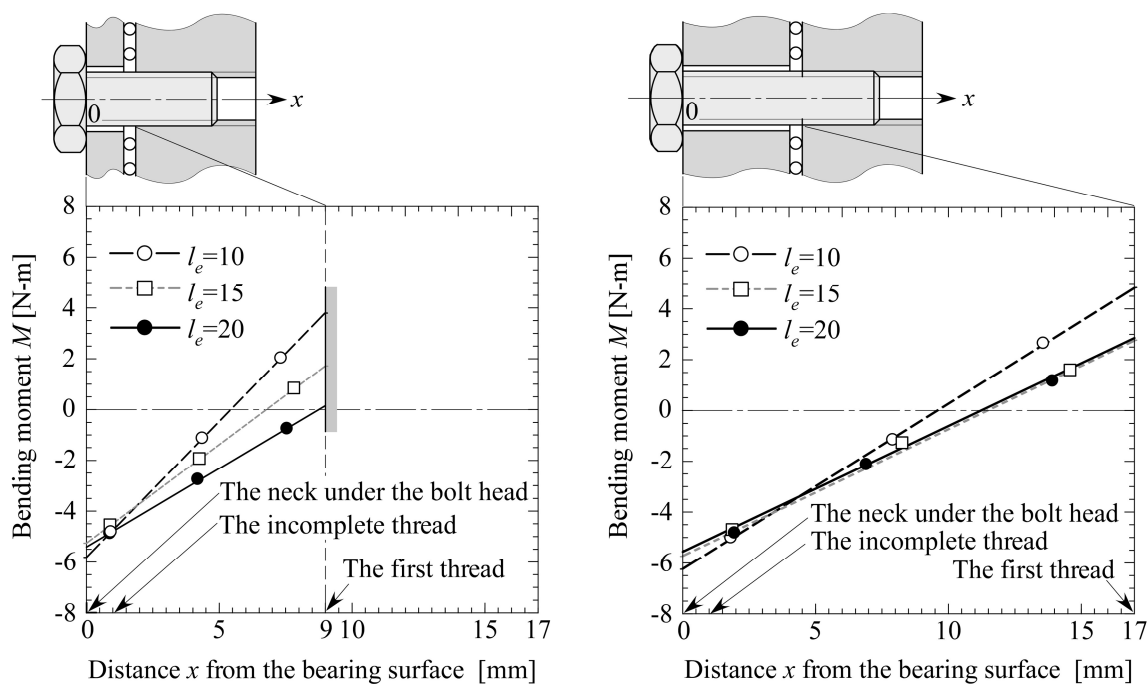


Fig. 9 - Relationships between apparent fatigue limits  $(\Delta P_t/2)_w$  and grip length  $l_e$  and fracture surfaces and typical fatigue cracks nucleated at the neck of bolt and at the incomplete thread of the bolt.

transverse fatigue limits  $(\Delta P_t/2)_w$  changed according to the engaging thread lengths  $l_e$  we measured the bending moment  $M(x)$  loaded on the bolt using strain gages.

Figure 10 shows the bending moments  $M(x)$  loaded on the bolts due to the transverse force  $\Delta P_t/2$ . Fig. 10(a) and (b) are the bending moment diagrams of the bolts with the grip length  $l_g=9$  mm and 17 mm respectively. In these figure, the ordinate is the bending moment  $M$  and the abscissa is the position  $x$  along the bolt axis. Points in the bending moment diagram indicates positions at which the bending moments were measured by strain gages.



(a) Bending moment diagram of the case for  $l_g=9$  mm (b) Bending moment diagram of the case for  $l_g=17$  mm

Fig. 10 - Bending moment diagrams acting on the test bolt with different grip lengths  $l_g$ .

It can be seen in Fig. 10 that the actual bending moments  $M(x)$  are linear functions as shown in Fig. 6 and are different according to the engaging thread length  $l_e$  and the grip length  $l_g$ . We discuss a relationship between the fracture position shown in Fig. 9(a) and the bending moment diagrams shown in Fig. 10.

The tightening conditions which the bolt broke at the root of incomplete thread are the case for  $l_e=15$  mm and 20 mm at  $l_g=9$  mm, and the case for  $l_e=15$  mm and 20 mm at  $l_g=17$  mm. It can be seen from the bending moment  $M$  at those cases that the bending moment  $M_{(RI)}$  at the root of the incomplete thread are higher than those  $M_{(RF)}$  at the root of the first thread. Therefore the amplitudes of cyclic maximum principal stress at the root of the incomplete thread become larger than those at the root of the first thread.

As the results, the bolt broke at the root of the incomplete thread. In the case for  $l_e=10$  mm at  $l_g=9$  mm, the bolt broke at the neck under the bolt head. It can be seen in Fig. 10(a) that gradient of the bending moment  $M$  was markedly large. Hence the difference between the bending moments  $M_{(RF)}$  at the root of the first thread and the bending moment  $M_{(RI)}$  at the root of the incomplete thread were large comparatively. Therefore the bolt broke at the neck under the bolt head although the section diameter at the neck under bolt head was large. In the case for  $l_e=10$  mm at  $l_g=17$  mm, the main fatigue cracks nucleated at the root of the incomplete thread and at the root of the first thread. It can be seen in Fig. 10(b) that the bending moment  $M_{(RF)}$  at the root of the first thread and the bending moments  $M_{(RI)}$  at the root of the incomplete thread were almost the same. Consequently the main fatigue cracks nucleated at the root of the incomplete thread and at the root of the first thread.

Incidentally, we focus on the results of the tightening cases for  $l_e=10$  mm and 20 mm in Fig. 9. The apparent transverse fatigue limit  $(\Delta P_t/2)_w$  significantly decreased with an increase in the engaging thread length  $l_e$ . And these main fatigue cracks of the broken bolt due to  $\Delta P_t/2$  just above  $(\Delta P_t/2)_w$  nucleated at the root of the incomplete thread and at the neck under the bolt head. To be realized this case, the bending moment at the first thread must decrease with an increase in the engaging thread length  $l_e$ . However if the engaging thread length is long, it is considered that the bolt thread is constrained strongly in the transverse direction. Hence we focus occurrence of inclination and slippage of the bolt thread due to the transverse vibration at the engaging threads. We investigated resistance force by friction to not slip at the engaging threads using FE analysis models shown in Fig. 11.

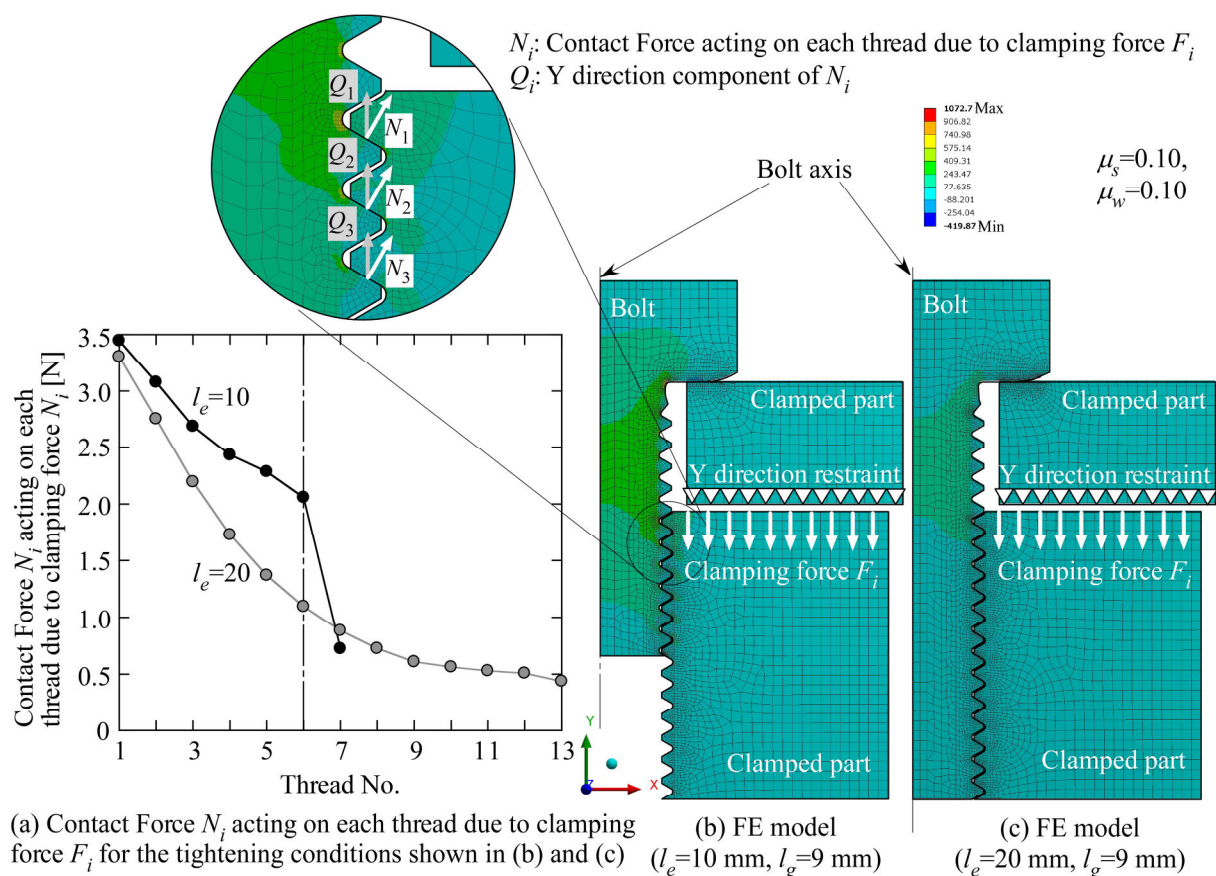


Fig. 11 - FE analysis model of the test bolts with different engaging thread lengths  $l_e$ .

Figure 11(a) shows the calculated contact forces  $N_i$  at each bolt thread of the bolts with  $l_e = 10$  mm and with  $l_e = 20$  mm. FE analysis was conducted with elastic axisymmetric model shown in Fig. 11(b) and (c). Fig. 11(b) shows the FE analysis models of the bolt with  $l_e = 10$  mm and Fig. 11(c) shows the FE analysis models of the bolt with  $l_e = 20$  mm. In the FE models, a lower surface of an upper clamped part was constrained in Y direction and clamping force  $F_i$  was applied to an upper surface of a lower clamped part. Young's modulus  $E$  and Poisson's ratio  $\nu$  of the bolt and the clamped parts were 206 GPa and 0.3 respectively. A friction coefficient between bearing surfaces  $\mu_w$  and a friction coefficient between thread surfaces  $\mu_s$  were assumed  $\mu_w = \mu_s = 0.10$ .

It can be seen in Fig. 11(a) that the contact force  $N_i$  of the bolts with  $l_e = 10$  mm is of course larger than that of the bolts with  $l_e = 20$  mm because the number of thread which loads the clamping force was small. If we assume that the first six threads mainly contribute to the inclination and the slippage at the engaging thread portion, the friction force  $P_{10}$  for  $l_e = 10$  mm becomes  $P_{10} = 2.5$  kN and the friction force  $P_{20}$  for  $l_e = 20$  mm becomes  $P_{20} = 2.0$  kN. Hence it can be considered that the inclination and the slippage at the engaging bolt thread of the bolted joint with  $l_e = 10$  mm is unlikely to occur. As the results, since the inclination and the slippage at the engaging bolt thread of the bolted joint with  $l_e = 20$  mm was likely to occur, it is considered that the apparent transverse fatigue limit  $(\Delta P_t/2)_w$  of the bolted joint with  $l_e = 20$  mm was lower than that  $(\Delta P_t/2)_w$  of the bolted joint with  $l_e = 10$  mm.

## CONCLUSION

In this study, transverse fatigue tests of the bolted joints with comparatively short grip length to simulate a thin plate structure have been conducted. The main conclusions obtained in this study are summarized as follows.

1. We investigated influence of the grip length on the apparent fatigue limit for the bolted joint with the engaging thread length 15 mm. Within the grip lengths 9 mm, 12 mm, 17 mm and 22 mm, the apparent transverse fatigue limits were in completely proportion to the grip length.
2. We also investigated influences of the engaging thread length on the apparent fatigue limits for the bolted joint with the grip length 9 mm and 17 mm. Within the engaging thread lengths 10 mm, 15 mm and 20 mm, the apparent transverse fatigue limits decreases with an increase in the engaging thread lengths. However the relationships were not linear.
3. The influence of the engaging thread lengths on the apparent transverse fatigue limits are magnified if the grip length was short.

## REFERENCES

[1]-Ministry of Land, Infrastructure and Transport, Press release report, The number of accidents that wheels fallen off by wheel bolt failure in 2010 is 24., [http://www.mlit.go.jp/report/press/jidosha09\\_hh\\_000039.html](http://www.mlit.go.jp/report/press/jidosha09_hh_000039.html), (accessed on 30 November, 2013) (in Japanese).

- [2]-Asahi Shinbun, News paper morning edition, March 19<sup>th</sup> 2002, 2002, p.35 (in Japanese).
- [3]-Kasei, S., Ishimura, M., and Ohashi, N., On Self-loosening of Threaded Joints in the Case of Absence of Macroscopic Bearing-surface Sliding, Bulletin of Japan Society of Precision Engineering, Vol. 23, 1989, pp.31-36 (in Japanese).
- [4]-Hess, D.P., Threaded Components under Axial Harmonic Vibration: Part 2-Kinematic Analysis, ASME Journal of Sound and Vibration, Vol-210, 1996, pp.255-265.
- [5]-Hess, D.P., and Sudhirkashyap, S.V., Dynamic Loosening and Tightening of a Single-bolt Assembly, ASME Journal of Vibration and Acoustics, Vol-119, 1997, pp.311-316.
- [6]-Pai, N.G. and Hess, D.P., Three-Dimensional Finite Element Analysis of Threaded Fastener Loosening due to Dynamic Shear Load, Engineering Failure Analysis, Vol-9, 2002, pp.383-402.
- [7]-Jiang, Y., Zhang, M., and Lee, C.-H., “A Study of Early Stage Self-loosening of Bolted Joints”, ASME *Journal of Mechanical Design*, Vol. 125, 2003, pp.518-526.
- [8]-Zhang, M., Jiang, Y., and Lee, C.-H., “An Experimental Investigation of the Effects of Clamped Length and Loading Direction on Self-Loosening of Bolted Joints”, Transaction of ASME, *Journal of Pressure vessel Technology*, Vol. 128, 2006, pp.388-393.
- [9]-Stephens, I., Bradley, J., Horn, J., Arkema, M. and Gradman, J., Influence of cold rolling threads before or after heat treatment on the fatigue resistance of high strength coarse thread bolts for multiple preload conditions, ASTM Special Technical Publication Vol.1487 STP, 2007, Pages 29-41
- [10]-Alexander, D.F., Skochko, G.W., Andrews, W.R., Briody, R.S., Fatigue testing of low-alloy steel fasteners subjected to simultaneous bending and axial loads, ASTM Special Technical Publication Issue 1391, 2000, pp. 72-84.
- [11]-Yoshimoto, I., Maruyama, K. and Yamada, Y., Prediction of Fatigue Strength of Bolt-nut Joints Based on Residual Stress, Transactions of the Japan Society of Mechanical Engineers, Series A, Vol.50, No.452 (1984), pp.717-721 (in Japanese).
- [12]-Ohashi, N., Hagiwara, M., and Yoshimoto, I., Characteristics of Bolted Joint in Plastic Region Tightening - Dispersion of Tightening Axial Force and Safety against Fatigue -, Bulletin of Japan Society of Precision Engineering, Vol. 51, No. 7, 1985, pp.31-36 (in Japanese).
- [13]-Ohashi, N., Kasano, H., and Yoshimoto, I., Research on Fatigue Testing of Bolts for Quality Assurance, Transactions of the Japan Society of Mechanical Engineers, Series C, Vol.60, No.576 (1994), pp.2879-2884 (in Japanese).
- [14]-Hashimura, S. and Darrell F. Socie, A Study of Loosening and Fatigue of Bolted Joints under Transverse Vibration, SAE 2005 Transactions, Journal of Materials and Manufacturing, Section 5, 2006, pp. 630-640.

[15]-Hashimura, S., Influences of Various Factors of Bolt Tightening on Loosening-Fatigue Failure under Transverse Vibration, SAE 2007 Transactions, Journal of Materials and Manufacturing, Section 5, 2007, pp. 262-270.

[16]-Hashimura, S. and Kurakake, Y., A Study to Predict Fatigue Limits of Bolted Joints under Transverse Vibration, Proceedings of the 2010 SAE World Congress, Detroit, Michigan, April 14-16, 2010, Technical Paper No. 2010-01-0964.

[17]-Yamamoto, A., Principle and Design for Bolted Joint Tightening, Yokendo Co-ltd, 1995, pp.147-178 (in Japanese).